ACCOUNTS
of chemical research

Designing Micro- and Nanoswimmers for Specific Applications

Jaideep Katuri,[†,‡] Xing Ma,[‡,§] Morgan M. Stanton,[‡] and Samuel Sánchez[*,†,‡,∥]

[†]Institute for Bioengineering of Catalonia (IBEC), Baldiri i Reixac 10-12, 08028 Barcelona, Spain
[‡]Max-Planck-Institut für Intelligente Systeme, Heisenbergstr. 3, D-70569 Stuttgart, Germany
[§]School of Materials Science and Engineering, Harbin Institute of Technology Shenzhen Graduate School, 518055 Shenzhen, China
[∥]Institució Catalana de Recerca i Estudis Avancats (ICREA), Pg. Lluís Companys 23, 08010 Barcelona, Spain

CONSPECTUS: Self-propelled colloids have emerged as a new class of active matter over the past decade. These are micrometer sized colloidal objects that transduce free energy from their surroundings and convert it to directed motion. The self-propelled colloids are in many ways, the synthetic analogues of biological self-propelled units such as algae or bacteria. Although they are propelled by very different mechanisms, biological swimmers are typically powered by flagellar motion and synthetic swimmers are driven by local chemical reactions, they share a number of common features with respect to swimming behavior. They exhibit run-and-tumble like behavior, are responsive to environmental stimuli, and can even chemically interact with nearby swimmers. An understanding of self-propelled colloids could help us in understanding the complex behaviors that emerge in populations of natural microswimmers. Self-propelled colloids also offer some advantages over natural microswimmers, since the surface properties, propulsion mechanisms, and particle geometry can all be easily modified to meet specific needs.

From a more practical perspective, a number of applications, ranging from environmental remediation to targeted drug delivery, have been envisioned for these systems. These applications rely on the basic functionalities of self-propelled colloids: directional motion, sensing of the local environment, and the ability to respond to external signals. Owing to the vastly different nature of each of these applications, it becomes necessary to optimize the design choices in these colloids. There has been a significant effort to develop a range of synthetic self-propelled colloids to meet the specific conditions required for different processes. Tubular self-propelled colloids, for example, are ideal for decontamination processes, owing to their bubble propulsion mechanism, which enhances mixing in systems, but are incompatible with biological systems due to the toxic propulsion fuel and the generation of oxygen bubbles. Spherical swimmers serve as model systems to understand the fundamental aspects of the propulsion mechanism, collective behavior, response to external stimuli, etc. They are also typically the choice of shape at the nanoscale due to their ease of fabrication. More recently biohybrid swimmers have also been developed which attempt to retain the advantages of synthetic colloids while deriving their propulsion from biological swimmers such as sperm and bacteria, offering the means for biocompatible swimming. In this Account, we will summarize our effort and those of other groups, in the design and development of self-propelled colloids of different structural properties and powered by different propulsion mechanisms. We will also briefly address the applications that have been proposed and, to some extent, demonstrated for these swimmer designs.

■ INTRODUCTION

Micromotors are small autonomous devices that are capable of performing complex tasks in fluidic environments. Since their first demonstration in 2004, there have been significant advances in terms of developing new propulsion mechanisms and in incorporating methods of motion control. The efforts to gain a deeper understanding of the physical mechanisms involved and attempts to use these micromotors in industrial and biomedical processes have largely occurred in parallel.

Among the first artificial micromotors developed were the bimetallic rods of Au−Pt, which propelled in a solution of H_2O_2 due to electrokinetic forces setup by the preferential oxidation of the peroxide on the Pt side and the reduction on the Au side.[1,2] Later on, two other geometries were demonstrated in spherical swimmers half coated with a metal catalyst to enable self-phoresis[3] and tubular structures, which had the catalyst on the inside and propelled due to the expulsion of oxygen bubbles.[4] Since then, a number of new propulsion methods have been developed for these micromotors including those based on photochemical, ultrasound, and thermophoretic mechanisms.[5] This range of geometries and propulsion mechanisms allows for a wide range of applications from biosensing and drug delivery to environmental remediation.[6−12]
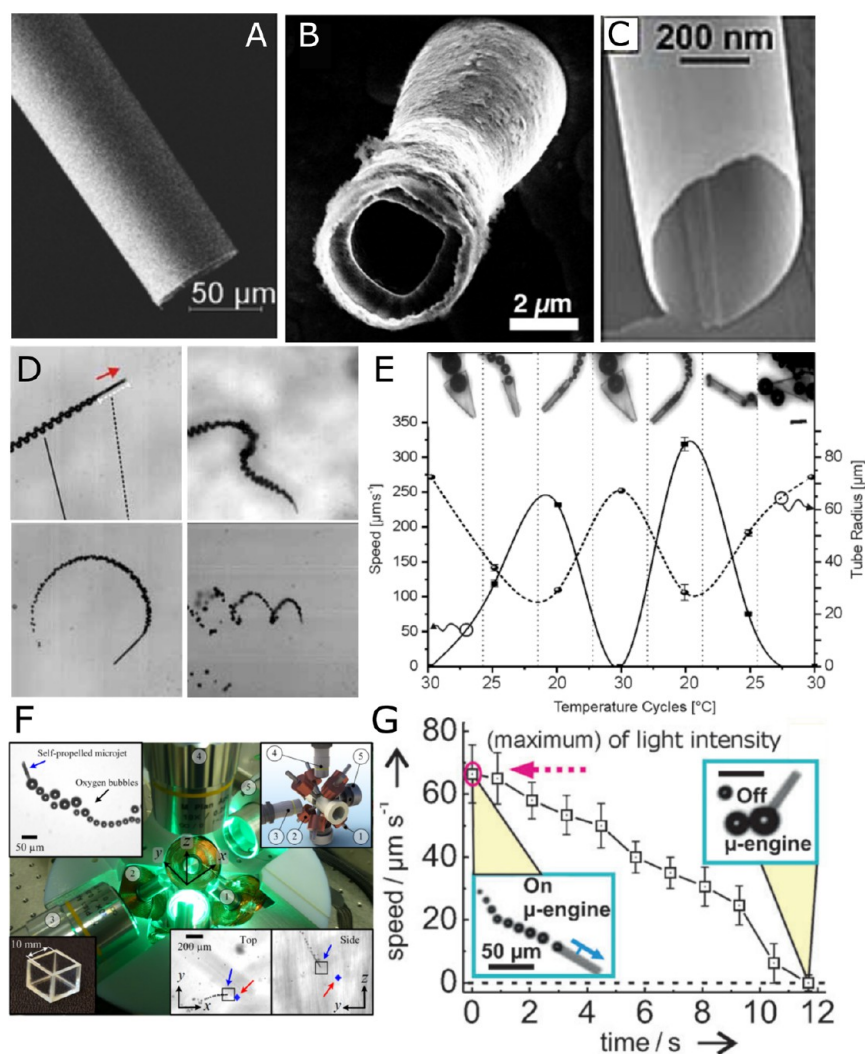
Figure 1. Fabrication and control of tubular microjets. SEM image of (A) a tubular microjet fabricated by the roll-up method, (B) a tubular microjet fabricated by electrodeposition method, and (C) a nanojet synthesized based on heteroepitaxically grown layers. (D) Different types of swimming behavior. (E) Folding and unfolding of thermoresponsive microtubes leads to a variation in propulsion velocities. (F) An eight-coil magnetic setup used for 3-D control of microjets. (G) Light regulated velocity control of microjets. Panel A reprinted with permission from ref 39. Copyright 2016 John Wiley and Sons, Inc. Panel C reprinted with permission from ref 24. Copyright 2011 John Wiley and Sons, Inc. Panel D reprinted with permission from ref 20. Copyright 2009 John Wiley and Sons, Inc. Panel E reprinted with permission from ref 23. Copyright 2014 John Wiley and Sons, Inc. Panel G reprinted with permission from ref 28. Copyright 2011 John Wiley and Sons, Inc. Panel F reprinted with permission from ref 27. Copyright 2013 AIP Publishing.

A major drawback, nevertheless, has been the toxicity of the fuel, making difficult the implementation of micromotors in biological systems. This challenge has been addressed by developing zinc and magnesium based micromotors, which can propel in nontoxic fuels or fuel free micromotors driven by light or magnetic fields.[13−16] Recent efforts have also focused on developing bubble-free enzyme based motors that derive their propulsion from biocompatible substrates, and biohybrid micromotors whose propulsion is driven by natural micro-swimmers such as sperms and bacteria. The flexibility that researchers have in controlling the physical properties of the micromotors makes them promising tools for a number of applications.

■ TUBULAR BUBBLE PROPELLED MICROJETS

Artificial microjets, based on microtubular geometries self-propel by the ejection of a jet of bubbles. These structures are fabricated by two main methods, roll-up nanotechnology[4,17]

and electrodeposition using porous templates.[18,19] Both methods incorporate a catalyst in the interior that decomposes the chemical substrate into gas bubbles (e.g., O_2 or H_2) (Figure 1A).[20,13] The microjets also require surfactants within the solution to reduce the surface tension in the tubular confinement, facilitating the stability and the release of bubbles.[21,22] The curvature and confinement of the microtube is crucial for the gas to accumulate and be used for propulsion.[23]

Electrodeposited microjets are smaller ($L \approx 5-10$ μm) (Figure 1B) than rolled-up microjets ($L \approx 25-500$ μm) and present a relative speed (body length (bl)·s^{-1}) larger than those observed in rolled-up tubes for the same concentration of fuel, reaching a maximum speed of 2400 μm s^{-1} in 5 wt % H_2O_2.[18] High-strain engineering with epitaxial growth of nanomem-branes can lead to nanojets of extremely small sizes, down to 280 nm in diameter (Figure 1C).[24]
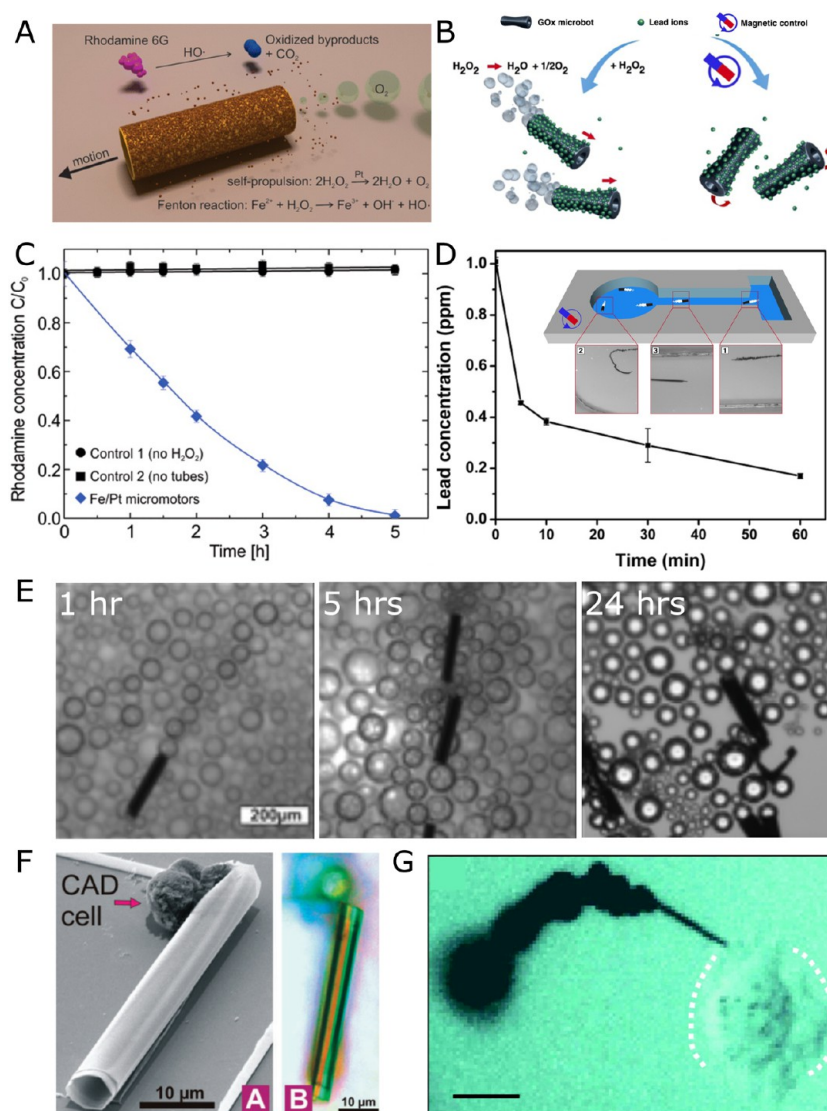
Figure 2. Environmental and biomedical applications of microjets. (A) Schematic for the degradation of polluted water (Rh6G) into inorganic products. (B) Scheme of graphene-oxide (GOx) microbots for lead decontamination and recovery. (C) Degradation of Rh6G (blue diamonds). Black dots and squares are controls. (D) Removal of lead by GOx micromotors. (E) Lifetime activity of microjets for 24 h. (F) SEM (A) and optical (B) images of a microjet with CAD cells. (G) Optical microscopy image of a nanotool drilling into a HeLa cell. Scalebar represents 10 μm. Panels A and C reprinted with permission from ref 35. Copyright 2013 American Chemical Society. Panels B and D reprinted with permission from ref 40. Copyright 2016 American Chemical Society. Panel G reprinted with permission from ref 25 Copyright 2012 American Chemical Society. Panel F reproduced with permission from ref 31, 2010 Royal Society of Chemistry.

The direction of motion of microjets cannot be, a priori, predicted. Small asymmetries can change the angle at which the bubbles are released, which contributes to a torque leading to trajectories of different shapes and speeds (Figure 1D,E).[25,26] To control their directionality in 3D,[27] various methods using magnetic fields, ultrasound, temperature, light, and chemical gradients have been presented (Figure 1, panels F[27] and G[28]) (see ref 6 and references therein).

The bubble-propelled microjets can swim in high ionic media unlike self-ionic diffusiophoretic and electrokinetic swimmers and in several different media, types of water, serum, and reconstituted blood (see ref 6 and references therein). Yet, small changes in viscosity of the medium affect the dynamics of the microjets. Their motion in reconstituted blood was hindered at 25 °C but was regained at physiological temperature, which reduced the viscosity of the media.[29,30]

Over the past few years, several proof-of-concept applications of microjets have been reported, including the drilling of soft matter[25] (Figure 2G), transport of cargo and cells on-chip[31−33] (Figure 2 F), biosensing,[34] and cleaning of polluted water.[35,36] However, the high concentration of H_2O_2 used for the propulsion causes oxidative stress, damaging and killing the cells. To address this limitation, more efficient and biocompatible means of propulsion are being developed. The use of enzymes[37] or motile cells[38] could give rise to biologically friendly micromotors and will be discussed in a later section.

Recent works have demonstrated that the bubbles released from the microjets can mix solutions and enhance chemical reactions. Microjets that use up H_2O_2 as a fuel and generate and actively transport free radicals in the solution in a 3D manner boost the degradation of organic dyes via Fenton-like reactions (Figure 2A,C). Long-term activity was recorded for rolled-up microjets as they continuously generated bubbles for 24 h
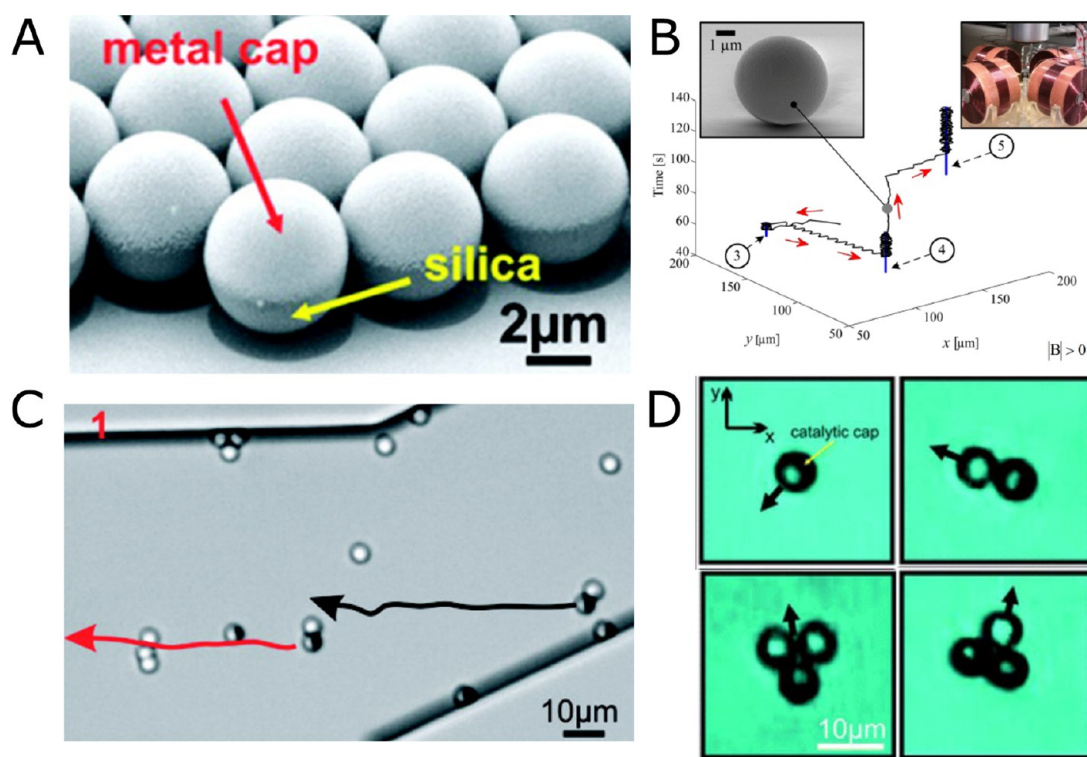
Figure 3. Self-phoretic Janus microswimmers. (A) SEM image of silica−Pt Janus particles. (B) External magnetic fields to guide particles. (C) Magnetic caps used to transport paramagnetic particles. (D) Transport of cargo by single/double Janus particle configuration. Panels A and C reproduced with permission from ref 44. Copyright 2012 American Chemical Society. Panel B reproduced with permission from ref 45. Copyright 2015 Intech. Panel D reproduced with permission from ref 46. Copyright 2011 Royal Society of Chemistry.
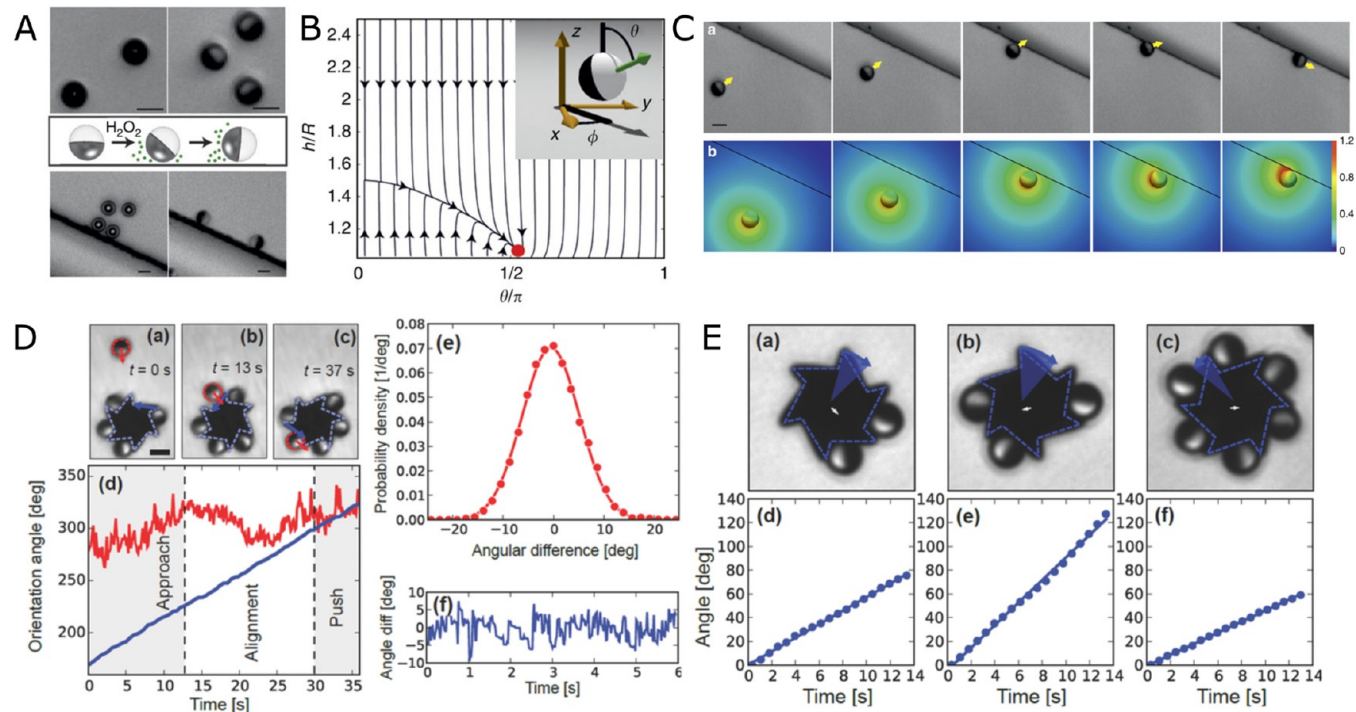

Figure 4. Self-phoretic Janus microswimmers near surfaces. (A) Silica−Pt Janus particles confined near a surface reorient on addition of H_2O_2. A second vertical step has similar effect. (B) Phase portrait of a Janus particle near a surface showing the steady-state at the cap-parallel position. (C) (a) Approach, reorientation, and guiding of a Janus particle at a vertical 800 nm step. (b) Numerically calculated steady-state distribution of the reaction products. (D) Self-assembly of Janus microswimmers around an asymmetric gear. (E) Dependence of angular velocity of the microgears on the number of Janus particles. Panels A−C reproduced with permission from ref 47. Copyright 2016 Nature Publishing Group. Panels D and E reproduced with permission from ref 48. Copyright 2016 John Wiley & Sons, Inc.
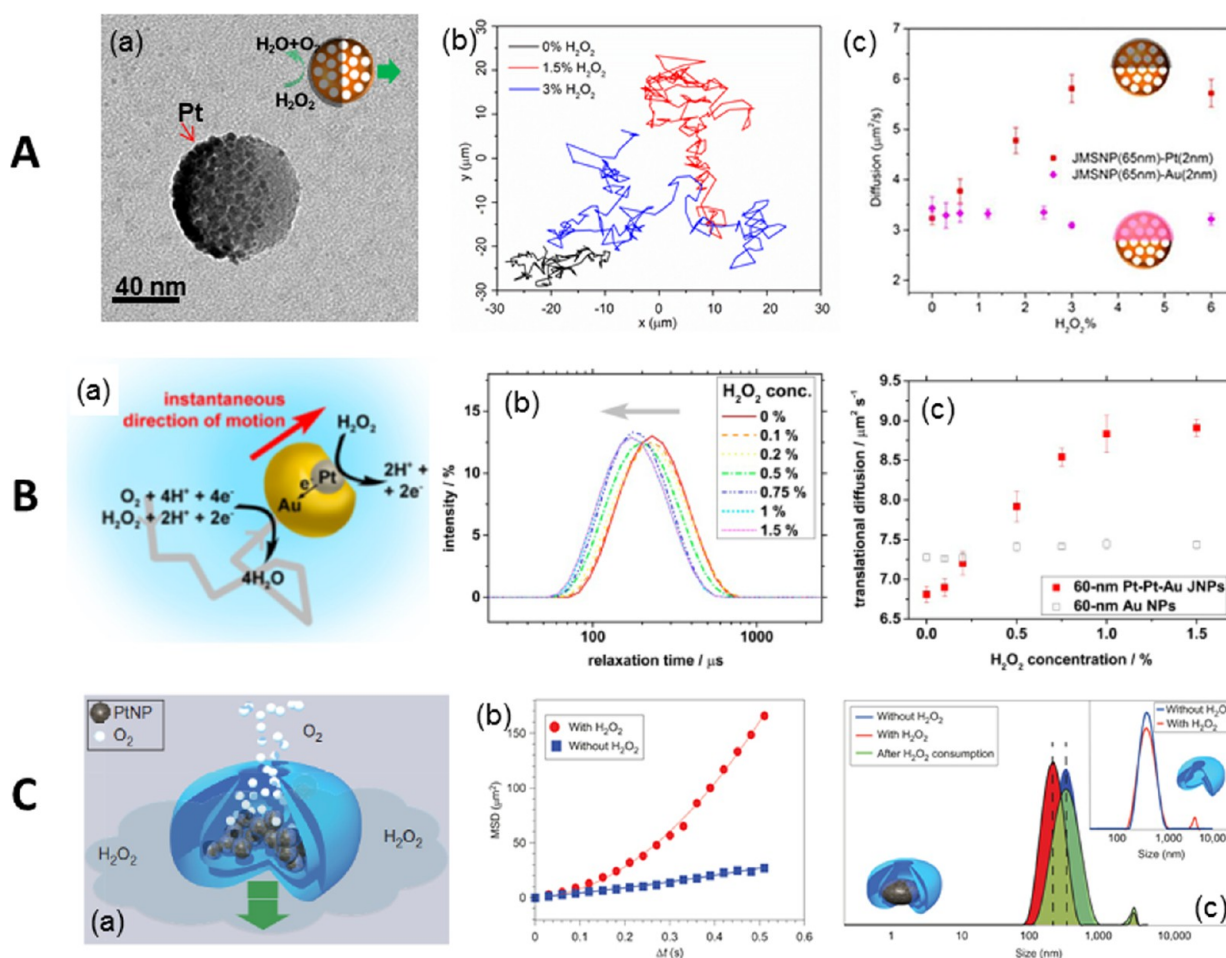
Figure 5. Propulsion at nanoscale. (A) Janus mesoporous silica nanomotor: (a) TEM image and schematic of the nanomotor, (b) tracking trajectories and (c) MSD plots of the nanomotors. (B) Au−Pt nanomotor: (a) schematic of the self-electrophoresis of Au−Pt nanomotor; DLS measurement indicates (b) a left shift of relaxation time and (c) enhancement of translational diffusion with increasing H_2O_2 concentration. (C) (a) Schematic of a stomatocytes nanomotor, (b) MSD of the platinum-filled stomatocytes before and after the addition of H_2O_2, and (c) size distribution of platinum-filled stomatocytes before (blue) and after (red) the addition of H_2O_2. Inset shows the same measurements for stomatocytes without Pt. Panel A reprinted with permission from ref 51. Copyright 2015 American Chemical Society. Panel B reprinted with permission from ref 52. Copyright 2014 American Chemical Society. Panel C reprinted from ref 53 with permission. Copyright 2012 Nature Publishing Group.

(Figure 2 E). These microjets can be reused over a couple of months without significant reduction in performance.[39] Electrodeposited microjets containing graphene-oxide on the outside[41] have been reported as "heavy metal scrubbers".[40] Pb is captured by graphene-modified microjets and cleaned out from contaminated solutions. The metal can thereafter be desorbed, and microjets can be reused again. (Figure 2B,D). These recent works demonstrate that despite the challenges in using microjets for biomedical applications, there is a possibility to use the chemical self-propulsion of microjets for other industrial applications.

■ SPHERICAL PHORETIC MICROSWIMMERS

To understand the fundamental aspects of directed motion at the micro- and nanoscale, spherical, phoretically propelled colloids have been preferred due to both the ease of fabrication for experimental studies and the convenience of modeling simpler geometries. In 2007, it was demonstrated by Howse et al. that colloidal particles half coated with Pt could undergo phoretic migration in local, self-generated chemical gradients.[3] When these particles are suspended in H_2O_2, the Pt half catalyzes the degradation of the peroxide while the silica half

remains inert. This creates a gradient of the reaction product around the colloidal particle in which the particle migrates. The exact details of the propulsion mechanism are still under debate because recent experiments suggested that the mechanism is perhaps more complex than the neutral diffusiophoretic model that was originally used to explain this behavior.[42,43]

Because of the microscale size of the Janus particles, they are subject to rotational diffusion due to thermal forces, which constantly reorient them. A method to control the directionality of the particles involves the use of out-of-plane magnetic layers together with catalytic layers. (Figure 3A,B).[44,45] It was also shown that Janus colloids (Figure 3C) could pick up and transport cargo via either magnetic or steric interactions (Figure 3D).[46]

Since the Janus particles swim close to surfaces, additional confinement effects become relevant, leading to a rich behavior of swimming.[49] Recent studies have shown that a combination of hydrodynamic, phoretic, and chemo-osmotic effects result in a stable orientation of the particles near surfaces.[47,50] When the particles are suspended in water, they orient with their caps facing the bottom surface due to the bottom heaviness induced by the Pt cap. However, once H_2O_2 is added to the system,

introducing activity, they assume a stable orientation that is parallel to the bottom surface (Figure 4A,B). It could also be shown, both experimentally and via numerical simulations, that the presence of a second perpendicular wall has a similar effect on the orientation of the particles. In proximity of a perpendicular wall, which could be as small as 400 nm step ($<0.2R_{particle}$), the particles tend to assume a stable orientation that is parallel to both the bottom surface and the perpendicular step (Figure 4C). This allows for the development of intrinsic guidance systems that do not rely on any external fields.

The ability of Janus particles to align and move along steps has also been exploited to assemble multiple particles around a microfabricated gear shaped structure, which has six asymmetric teeth and an external radius of 8 μm (Figure 4D).[48] Initially the Janus particles and the gears are suspended in water where they are randomly distributed. Upon addition of H_2O_2, the particles begin to self-propel while the passive gears remain inert. When a particle approaches the gear, it aligns along the edge of the gear and depending on the angle of incidence either leaves the gear or slides to the corner where it gets stuck (Figure 4D(a–d)). The effect of the number of self-propelled particles assembled around a gear and its angular velocity was also studied. It could be shown that up to three particles, the angular velocity increases on addition of new self-propelled particles. However, an even greater number of particles results in lower angular velocities probably owing either to the local depletion of fuel concentration around the gear or the chemical gradient from adjacent particles resulting in lower propulsion velocities (Figure 4E).

■ SWIMMING AT THE NANOSCALE

Achieving directional propulsion of nanomotors is challenging due to the strong rotational diffusion at these length scales. The nanomotors possess very short persistence length ($L = \tau V$, where τ is the rotational diffusion time and V is the ballistic velocity), which is difficult to observe by optical microscopy techniques.[54] Usually, the self-propelled nanomotors are characterized by the enhancement of effective diffusion coefficient (D_{eff}).

A series of half-coated catalytic Janus mesoporous silica nanomotors with an average diameter of 40, 65, and 90 nm (Figure 5A, part a) could be propelled by the heterogeneous catalytic reaction of H_2O_2 decomposition and driven by a self-diffusiophoretic mechanism. Tracking trajectories of these nanomotors (90 nm) demonstrated a larger diffusion in the presence of H_2O_2 (blue and red) compared to that without it (black) (Figure 5A, part b).[51] Another type of nanomotor based on Au–Pt metals was fabricated by the glancing angle deposition method (GLAD) with sizes of 30 or 60 nm. Their motion mechanism was attributed to self-electrophoresis due to charge transfer induced electric field (Figure 5B, part a). Dynamic light scattering (DLS) experiments showed a fuel dependent "left-shift" behavior in the distribution curve of the relaxation time of Au–Pt nanomotors (Figure 5B, part b), corresponding to an enhancement of effective diffusion coefficient (Figure 5B, part c).[52] Nanomotors based on supramolecular self-assembly loaded with Pt NPs (Figure 5C, part a) also show enhanced diffusion in the presence of H_2O_2 (Figure 5C, parts b and c). Nanoparticle tracking analysis (NTA) technology was used for tracking of the nanomotors, and their motion was attributed to a fast ejection of catalytic reaction products, for example, O_2, from the small opening of the stomatocytes.[53]

To move toward more biocompatible propulsion sources, there has been a recent effort to integrate enzymes in the nanomotors.[55] Enzymes trigger biocatalytic reactions, which can convert chemical energy into kinetic motion for bioprocesses, for example, intracellular protein transport. Researchers immobilized catalase into "roll-up" microtubes providing efficient bubble propulsion (about 10 times faster propulsion than with Pt catalyst) by triggering the decomposition of H_2O_2 inside the microjets (Figure 6A, part a).[37] A
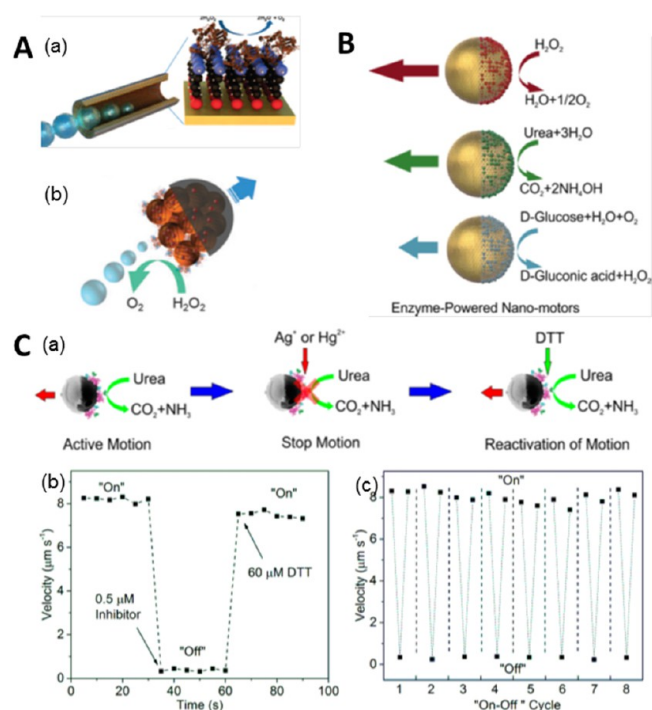

Figure 6. Enzyme-powered micro- and nanomotors. (A) Bubble propulsion of (a) tubular microjet and (b) Janus mesoporous cluster motor modified with catalase. (B) Self-propulsion of Janus hollow mesoporous nanomotors powered by various enzymes, catalase, urease, and glucose oxidase (GOx). (C) Urease powered hollow capsule: (a) motion control by manipulating the enzymatic activity, (b) "on"/"off" motion control by addition of inhibitor and DTT, and (c) repeated motion control up to 8 cycles. Panel A, part a, reproduced with permission from ref 37. Copyright 2010 American Chemical Society. Panel A, part b, reprinted with permission from ref 56. Copyright 2015 Royal Society of Chemistry. Panel B reproduced with permission from ref 57. Copyright 2015 American Chemical Society. Panel C reprinted with permission from ref 58. Copyright 2016 American Chemical Society.

similar strategy has been employed to power polymeric microtubes fabricated by template assisted electrochemistry deposition[59] or layer-by-layer self-assembly.[60] In smaller motors, catalase was also recently conjugated onto one side of a Janus mesoporous silica cluster, and its propulsion was driven by continuous generation of O_2 bubbles. (Figure 6A, part b).[56]

One advantage of enzyme powered micro- or nanomotors is the versatility in choices of enzyme/fuel combinations. Janus structures of hollow mesoporous silica nanoparticles were coupled with catalase, urease, and glucose oxidase (GOx) to achieve propulsion (Figure 6 B).[57] On a slightly larger scale, fuel dependent enhanced diffusion of polystyrene microparticles fully coated with catalase or urease enzymes has
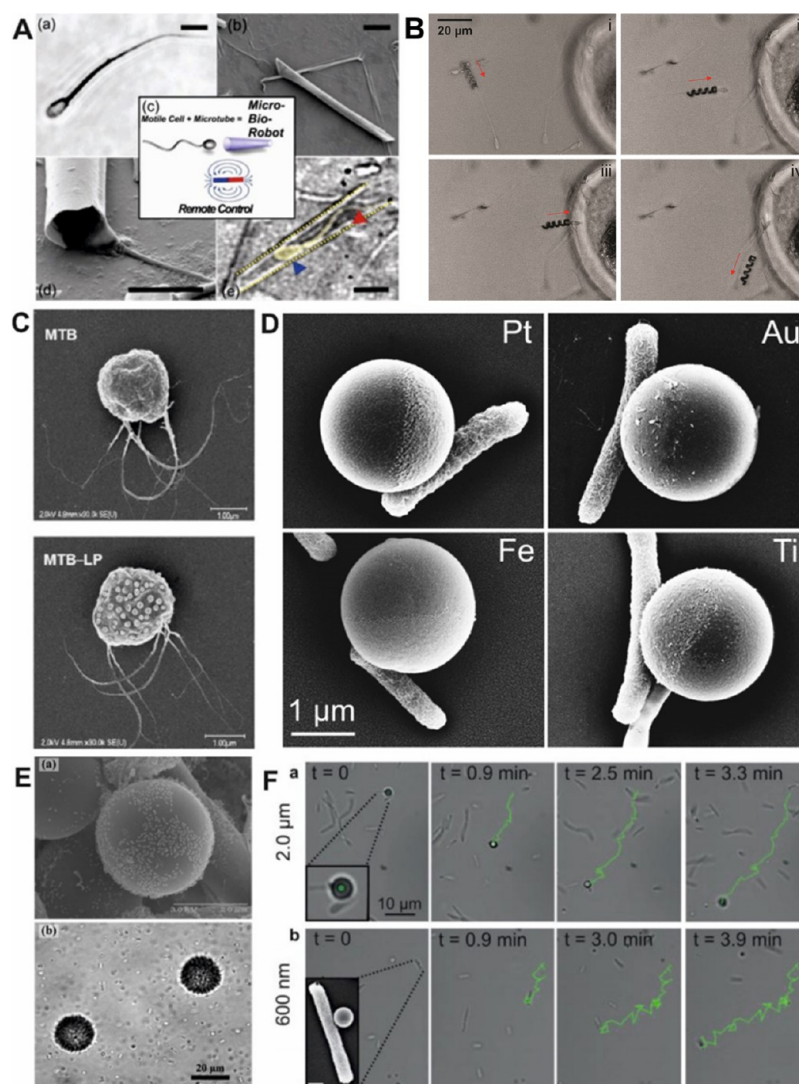
Figure 7. Sperm and bacteria powered biohybrids. (A) Bull spermatoozen trapped within microtubes. (B) Sperm cell coupling (i), transport (ii), approach to the oocyte membrane (iii), and release (iv). (C) MC-1 bacteria with (bottom) and without liposomes (top). (D) Janus particles with specific cell adhesion of *E. coli* to the metal cap. (E) Beads (30 μm) with attached *Serratia marcescens*. (F) Examples of *E. coli* swimming with 2 μm and 600 nm Janus particles. Panels A, D, and F reprinted with permission from refs 38 and 76. Copyright 2016 John Wiley and Sons, Inc. Panel B reprinted with permission from ref 69. Copyright 2016 American Chemical Society. Panel C reprinted with permission from ref 72. Copyright 2014 American Chemical Society. Panel E reprinted with permission from ref 75. Copyright 2012 Springer Science+Business Media, LLC.

been reported.[61] Polymeric stomatocyte nanoparticles were loaded with catalase and GOx, consuming glucose to achieve self-propulsion via a cascade of enzymatic reactions.[62] Enzymes were able to power nanorods,[63] nanotubes,[64] and Janus microparticles,[65] which all demonstrated enhanced diffusion as well. These works have demonstrated the feasibility of using biocompatible fuels, for example, urea and glucose, to power micro- and nanomotors. Moreover, long-range directional propulsion of enzymatic micromotors was recently reported for urease conjugated Janus structures of mesoporous silica hollow particles (Figure 6C, part a).[58] These self-propelled microcapsules were powered by urease triggered decomposition of urea at physiological concentrations. By manipulating the enzymatic activity of urease by addition of inhibitors, for example, Hg^{2+} or Ag^+, the motors could also be instantly stopped and, upon addition of the enzyme protection reagent dithiothreitol (DTT), reactivated (Figure 6C, part b) for multiple cycles (Figure 6C, part c). Additionally, incorporation of a magnetic element into the structure allows for directional guidance. Bubble-free propulsion of enzyme-powered tubular nanojets of 220 nm diameter and tunable lengths has been recently reported.[64] Biocompatible tubular nanojets and micro- and nanomotors hold great potential for active drug delivery *in vitro* and even *in vivo*.

■ BIOHYBRID MICROMOTORS

Biohybrid motors focus on the interaction of a motile cell with artificial materials to create a mobile system that is powered by cellular actuation. Biohybrids are not powered by toxic chemical fuels but by biological fluids, making them ideal for biomedical applications. They are responsive to their local environment (pH, temperature, and chemical gradients) and are capable of performing complex tasks that synthetic-only motors would not be capable of. For a biohybrid powered by a single flagellated cell, sperm are an optimal candidate. Sperm are powerful microscale (50−70 μm long) cells that have demonstrated directional guidance by chemotaxis, thermotaxis, and rheotaxis and can alter their flagella beat when exposed to chemical

signals. For a sperm powered microbot, a single bull spermatozoon was trapped within a fabricated microtube (20−50 μm) (Figure 7A).[38] The partial penetration of the sperm into the tube, allowed the flagellum to operate unhindered and push the tube through a fluid with an average velocity of 5−30 μm/s depending on the penetration depth, length of tube, and temperature. The magnetic properties of the microtube allowed for external magnetic guidance with a permanent magnet or an electromagnetic coil, and the biohybrid could be directed through a microfluidic chamber.[66,67] Triggered release of sperm from biohybrids was achieved with the thermoresponsive polymer poly(N-isopropylacrylamide) (PNIPAM) incorporated into flexible microtubes,[68] by increasing the temperature of the solution above 28 °C forcing the polymer microtube tube to unroll. More recently, a sperm biohybrid has been fabricated by capturing a sperm inside a microhelix.[69] Using direct laser writing,[70] microhelices that were capable of swimming with an applied rotating magnetic field were fabricated from a NiTi bilayer. The rotating helix delivered and released the sperm to an oocyte wall, suggesting the biohybrid's applicability for infertility treatment. However, the future of sperm biohybrids for fertilization applications will require testing these biohybrids in *in vivo* environments (Figure 7B).

For multiflagellated biohybrid systems, there have been significant developments of biohybrids using bacterial swimming power. Unlike sperm, bacteria occur in multiple areas of the human microbiome[71] making them more viable for variable biomedical applications. They are also significantly shorter in scale (0.7−7 μm long) compared to other bioactuators allowing them to navigate in smaller environments. Some of the smallest synthetic cargo delivered by bacteria include nanoscale liposomes (70 liposomes) bound to MC-1 magnetotactic bacteria (Figure 7C).[72] Once the biohybrid was incubated with mammalian cells (J774, NIH/3T3, and Colo205), the immobile cells could take up the swimming biohybrid with liposomes, exhibiting the biohybrid's potential ability as a drug carrying system. For development of biohybrids with larger cargo loads, bacteria coupled with nano- or microparticles have been investigated (Figure 7D,E). Initial work with bacteria−-particle swimmers attached *Serratia marcescens* to 10 μm polystyrene beads and achieved a biohybrid with an average velocity of 15 μm/s, but with random directionality.[73] A number of methods have been employed to guide bacteria biohybrid swimming, including chemotaxis,[74,75] pH taxis,[76] and specified cell adhesion for unified propulsion force.[77] For guided cell adhesion, directional swimming, and drug delivery, contained in a single biohybrid, a multifunctional biohybrid was developed.[78] Metal capped (Au, Pt, Fe, Ti) 2 μm and 600 nm polystyrene particles were coupled with *Escherichia coli* (*E. coli*) (Figure 7D,F). *E. coli* preferentially adhered only to the metal cap of the Janus particle without secondary surface modification[79] or antibodies[80] for simple and rapid biohybrid formation. The polystyrene side of the Janus particle was modified with the anticancer agent doxorubicin hydrochloride, demonstrating that the biohybrid was capable of directed cell adhesion and localized drug attachment. The preferential adhesion of the bacteria to the metal cap was found to be related to the hydrophobicity of the metal cap. Such bacteria biohybrids demonstrate how these systems are moving toward real-world applicability, but certain obstacles remain. Similar to the sperm biohybrids, bacteria biohybrids need more experimentation *in vivo* and sophisticated imaging techniques

to achieve controlled guidance. Materials and architectures, other than particles, should also be investigated for bacteria biohybrids;[81] this may lead to greater directional guidance and new opportunities for cargo delivery.

■ CONCLUSIONS

The interest in the field of artificial micro and nanomotors has grown steadily over the past decade. This has been both due to the greater physical understanding that we now have of these systems and the recent advances in nanotechnology, which let researchers create and test new designs of these motors. Some of these designs have been driven purely by our interest in creating biomimetic swimmers at the microscale such as asymmetric colloidal particles that are gravitactic, similar to paramecium, or rheotactic, akin to sperm and bacteria. Colloidal swimmers that sense and respond to each other via chemical fields were also realized mimicking population scale effects from the microbial world. Experiments with biomimetic colloidal microswimmers could enhance our understanding of the physical mechanisms involved in biological swimmers.

The other motivation for the design of micromotors is more practical, to develop autonomous microdevices that can perform useful tasks, either independently or in response to external signals. A number of applications have been demonstrated with these micromotors ranging from cargo delivery to environmental remediation and bio sensing. It is imperative in this case to have a design that is optimized for particular applications, provides for precise motion control, and is fully compatible with the system. The compatibility has been a significant challenge especially when it comes to biological applications, mostly due to the fuels, which are generally non-biocompatible. However, recent progress and current efforts to incorporate biological components such as enzymes and biological swimmers into synthetic micromotors seems to be addressing this problem in a significant way, opening up exciting areas of application for artificial micromotors.

■ AUTHOR INFORMATION

Corresponding Author

*E-mail: ssanchez@ibecbarcelona.eu.

Notes

The authors declare no competing financial interest.

Biographies

Jaideep Katuri received his M.Sc. in Physics from the University of Stuttgart, Germany, in 2015. He is currently working on his Ph.D. in the group of Prof. Sanchez at Institute for Bioengineering of Catalonia, Barcelona. His research interests are focused on studying the properties of active colloids near interfaces.

Xing Ma received his Ph.D. from Nanyang Technological University in 2013 and has been working as Alexander von Humboldt research fellow at Max-Planck Institute for Intelligent Systems at Stuttgart, Germany, since 2014. His research interest focuses on enzyme

powered mesoporous silica micro- and nanomotors for active drug delivery.

Morgan M. Stanton received her Ph.D. in Chemistry from Worcester Polytechnic Institute in Worcester, Massachusetts, U.S.A. in 2014. She is currently a postdoctoral fellow at the Max Planck for Intelligent Systems in Stuttgart, Germany. Her multidisciplinary research combines biology, chemistry, and materials science for the development of new biohybrids and biomaterials.

Samuel Sanchez is an ICREA Professor at the Institute for Bioengineering of Catalonia, Barcelona, and Group Leader at the Max Planck for Intelligent Systems in Stuttgart. His research interest focuses on different types of self-propelled micro- and nanobots, biosensors, and nanobiotechnology, among others.

■ REFERENCES

(1) Paxton, W. F.; Kistler, K. C.; Olmeda, C. C.; Sen, A.; St. Angelo, S. K.; Cao, Y.; Mallouk, T. E.; Lammert, P. E.; Crespi, V. H. Catalytic Nanomotors: Autonomous Movement of Striped Nanorods. *J. Am. Chem. Soc.* **2004**, *126*, 13424−13431.

(2) Wang, Y.; Hernandez, R. M.; Bartlett, D. J.; Bingham, J. M.; Kline, T. R.; Sen, A.; Mallouk, T. E. Bipolar Electrochemical Mechanism for the Propulsion of Catalytic Nanomotors in Hydrogen Peroxide Solutions. *Langmuir* **2006**, *22*, 10451−10456.

(3) Howse, J. R.; Jones, R. A. L.; Ryan, A. J.; Gough, T.; Vafabakhsh, R.; Golestanian, R. Self-Motile Colloidal Particles: From Directed Propulsion to Random Walk. *Phys. Rev. Lett.* **2007**, *99*, 048102.

(4) Mei, Y.; Solovev, A. A.; Sanchez, S.; Schmidt, O. G. Rolled-up Nanotech on Polymers: From Basic Perception to Self-Propelled Catalytic Microengines. *Chem. Soc. Rev.* **2011**, *40*, 2109−2119.

(5) Wang, W.; Duan, W.; Ahmed, S.; Mallouk, T. E.; Sen, A. Small Power: Autonomous Nano- and Micromotors Propelled by Self-Generated Gradients. *Nano Today* **2013**, *8*, 531−554.

(6) Sánchez, S.; Soler, L.; Katuri, J. Chemically Powered Micro- and Nanomotors. *Angew. Chem., Int. Ed.* **2015**, *54*, 1414−1444.

(7) Guix, M.; Mayorga-Martinez, C. C.; Merkoçi, A. Nano/Micromotors in (Bio)chemical Science Applications. *Chem. Rev.* **2014**, *114*, 6285−6322.

(8) Soler, L.; Sánchez, S. Catalytic Nanomotors for Environmental Monitoring and Water Remediation. *Nanoscale* **2014**, *6*, 7175−7182.

(9) Gao, W.; Wang, J. The Environmental Impact of Micro/Nanomachines: A Review. *ACS Nano* **2014**, *8*, 3170−3180.

(10) Wang, H.; Pumera, M. Fabrication of Micro/Nanoscale Motors. *Chem. Rev.* **2015**, *115*, 8704−8735.

(11) Wang, J. *Nanomachines: Fundamentals and Applications*; John Wiley & Sons: New York, 2013.

(12) Wang, J.; Gao, W. Nano/Microscale Motors: Biomedical Opportunities and Challenges. *ACS Nano* **2012**, *6*, 5745−5751.

(13) Gao, W.; Uygun, A.; Wang, J. Hydrogen-Bubble-Propelled Zinc-Based Microrockets in Strongly Acidic Media. *J. Am. Chem. Soc.* **2012**, *134*, 897−900.

(14) Gao, W.; Feng, X.; Pei, A.; Gu, Y.; Li, J.; Wang, J. Seawater-Driven Magnesium Based Janus Micromotors for Environmental Remediation. *Nanoscale* **2013**, *5*, 4696−4700.

(15) Dong, R.; Zhang, Q.; Gao, W.; Pei, A.; Ren, B. Highly Efficient Light-Driven TiO2−Au Janus Micromotors. *ACS Nano* **2016**, *10*, 839−844.

(16) Gao, W.; Kagan, D.; Pak, O. S.; Clawson, C.; Campuzano, S.; Chuluun-Erdene, E.; Shipton, E.; Fullerton, E. E.; Zhang, L.; Lauga, E.; Wang, J. Cargo-Towing Fuel-Free Magnetic Nanoswimmers for Targeted Drug Delivery. *Small* **2012**, *8*, 460−467.

(17) Mei, Y.; Huang, G.; Solovev, A. A.; Ureña, E. B.; Mönch, I.; Ding, F.; Reindl, T.; Fu, R. K. Y.; Chu, P. K.; Schmidt, O. G. Versatile Approach for Integrative and Functionalized Tubes by Strain Engineering of Nanomembranes on Polymers. *Adv. Mater.* **2008**, *20*, 4085−4090.

(18) Gao, W.; Sattayasamitsathit, S.; Orozco, J.; Wang, J. Highly Efficient Catalytic Microengines: Template Electrosynthesis of Polyaniline/Platinum Microtubes. *J. Am. Chem. Soc.* **2011**, *133*, 11862−11864.

(19) Zhao, G.; Pumera, M. Concentric Bimetallic Microjets by Electrodeposition. *RSC Adv.* **2013**, *3*, 3963−3966.

(20) Solovev, A. A.; Mei, Y.; Bermúdez Ureña, E.; Huang, G.; Schmidt, O. G. Catalytic Microtubular Jet Engines Self-Propelled by Accumulated Gas Bubbles. *Small* **2009**, *5*, 1688−1692.

(21) Wang, H.; Zhao, G.; Pumera, M. Crucial Role of Surfactants in Bubble-Propelled Microengines. *J. Phys. Chem. C* **2014**, *118*, 5268−5274.

(22) Simmchen, J.; Magdanz, V.; Sanchez, S.; Chokmaviroj, S.; Ruiz-Molina, D.; Baeza, A.; Schmidt, O. G. Effect of Surfactants on the Performance of Tubular and Spherical Micromotors − a Comparative Study. *RSC Adv.* **2014**, *4*, 20334−20340.

(23) Magdanz, V.; Stoychev, G.; Ionov, L.; Sanchez, S.; Schmidt, O. G. Stimuli-Responsive Microjets with Reconfigurable Shape. *Angew. Chem.* **2014**, *126*, 2711−2715.

(24) Sanchez, S.; Solovev, A. A.; Harazim, S. M.; Deneke, C.; Feng Mei, Y.; Schmidt, O. G. The Smallest Man-Made Jet Engine. *Chem. Rec.* **2011**, *11*, 367−370.

(25) Solovev, A. A.; Xi, W.; Gracias, D. H.; Harazim, S. M.; Deneke, C.; Sanchez, S.; Schmidt, O. G. Self-Propelled Nanotools. *ACS Nano* **2012**, *6*, 1751−1756.

(26) Solovev, A. A.; Sanchez, S.; Pumera, M.; Mei, Y. F.; Schmidt, O. G. Magnetic Control of Tubular Catalytic Microbots for the Transport, Assembly, and Delivery of Micro-objects. *Adv. Funct. Mater.* **2010**, *20*, 2430−2435.

(27) Khalil, I. S. M.; Magdanz, V.; Sanchez, S.; Schmidt, O. G.; Misra, S. Three-Dimensional Closed-Loop Control of Self-Propelled Microjets. *Appl. Phys. Lett.* **2013**, *103*, 172404.

(28) Solovev, A. A.; Smith, E. J.; Bof Bufon, C. C.; Sanchez, S.; Schmidt, O. G. Light-Controlled Propulsion of Catalytic Microengines. *Angew. Chem., Int. Ed.* **2011**, *50*, 10875−10878.

(29) Soler, L.; Martínez-Cisneros, C.; Swiersy, A.; Sánchez, S.; Schmidt, O. G. Thermal Activation of Catalytic Microjets in Blood Samples Using Microfluidic Chips. *Lab Chip* **2013**, *13*, 4299−4303.

(30) Sanchez, S.; Ananth, A. N.; Fomin, V. M.; Viehrig, M.; Schmidt, O. G. Superfast Motion of Catalytic Microjet Engines at Physiological Temperature. *J. Am. Chem. Soc.* **2011**, *133*, 14860−14863.

(31) Sanchez, S.; Solovev, A. A.; Schulze, S.; Schmidt, O. G. Controlled Manipulation of Multiple Cells Using Catalytic Microbots. *Chem. Commun.* **2011**, *47*, 698−700.

(32) Sanchez, S.; Solovev, A. A.; Harazim, S. M.; Schmidt, O. G. Microbots Swimming in the Flowing Streams of Microfluidic Channels. *J. Am. Chem. Soc.* **2011**, *133*, 701−703.

(33) Balasubramanian, S.; Kagan, D.; Jack Hu, C.-M.; Campuzano, S.; Lobo-Castañon, M. J.; Lim, N.; Kang, D. Y.; Zimmerman, M.; Zhang, L.; Wang, J. Micromachine-Enabled Capture and Isolation of Cancer Cells in Complex Media. *Angew. Chem., Int. Ed.* **2011**, *50*, 4161−4164.

(34) Campuzano, S.; Kagan, D.; Orozco, J.; Wang, J. Motion-Driven Sensing and Biosensing Using Electrochemically Propelled Nanomotors. *Analyst* **2011**, *136*, 4621−4630.

(35) Soler, L.; Magdanz, V.; Fomin, V. M.; Sanchez, S.; Schmidt, O. G. Self-Propelled Micromotors for Cleaning Polluted Water. *ACS Nano* **2013**, *7*, 9611−9620.

(36) Guix, M.; Orozco, J.; García, M.; Gao, W.; Sattayasamitsathit, S.; Merkoçi, A.; Escarpa, A.; Wang, J. Superhydrophobic Alkanethiol-Coated Microsubmarines for Effective Removal of Oil. *ACS Nano* **2012**, *6*, 4445−4451.

(37) Sanchez, S.; Solovev, A. A.; Mei, Y.; Schmidt, O. G. Dynamics of Biocatalytic Microengines Mediated by Variable Friction Control. *J. Am. Chem. Soc.* **2010**, *132*, 13144−13145.

(38) Magdanz, V.; Sanchez, S.; Schmidt, O. G. Development of a Sperm-Flagella Driven Micro-Bio-Robot. *Adv. Mater.* **2013**, *25*, 6581−6588.

(39) Parmar, J.; Vilela, D.; Pellicer, E.; Esqué-de los Ojos, D.; Sort, J.; Sánchez, S. Reusable and Long-Lasting Active Microcleaners for

Heterogeneous Water Remediation. *Adv. Funct. Mater.* **2016**, *26*, 4152−4161.

(40) Vilela, D.; Parmar, J.; Zeng, Y.; Zhao, Y.; Sánchez, S. Graphene-Based Microbots for Toxic Heavy Metal Removal and Recovery from Water. *Nano Lett.* **2016**, *16*, 2860−2866.

(41) Martín, A.; Jurado-Sánchez, B.; Escarpa, A.; Wang, J. Template Electrosynthesis of High-Performance Graphene Microengines. *Small* **2015**, *11*, 3568−3574.

(42) Ebbens, S.; Gregory, D. A.; Dunderdale, G.; Howse, J. R.; Ibrahim, Y.; Liverpool, T. B.; Golestanian, R. Electrokinetic Effects in Catalytic Platinum-Insulator Janus Swimmers. *EPL Europhys. Lett.* **2014**, *106*, 58003.

(43) Brown, A.; Poon, W. Ionic Effects in Self-Propelled Pt-Coated Janus Swimmers. *Soft Matter* **2014**, *10*, 4016−4027.

(44) Baraban, L.; Makarov, D.; Streubel, R.; Mönch, I.; Grimm, D.; Sanchez, S.; Schmidt, O. G. Catalytic Janus Motors on Microfluidic Chip: Deterministic Motion for Targeted Cargo Delivery. *ACS Nano* **2012**, *6*, 3383−3389.

(45) Khalil, I. S. M.; Magdanz, V.; Sanchez, S.; Schmidt, O. G.; Misra, S. Precise Localization and Control of Catalytic Janus Micromotors Using Weak Magnetic Fields. *Int. J. Adv. Robot. Syst.* **2015**, *12*, 1.

(46) Baraban, L.; Tasinkevych, M.; Popescu, M. N.; Sanchez, S.; Dietrich, S.; Schmidt, O. G. Transport of Cargo by Catalytic Janus Micro-Motors. *Soft Matter* **2012**, *8*, 48−52.

(47) Simmchen, J.; Katuri, J.; Uspal, W. E.; Popescu, M. N.; Tasinkevych, M.; Sánchez, S. Topographical Pathways Guide Chemical Microswimmers. *Nat. Commun.* **2016**, *7*, 10598.

(48) Maggi, C.; Simmchen, J.; Saglimbeni, F.; Katuri, J.; Dipalo, M.; De Angelis, F.; Sanchez, S.; Di Leonardo, R. Self-Assembly of Micromachining Systems Powered by Janus Micromotors. *Small* **2016**, *12*, 446−451.

(49) Uspal, W. E.; Popescu, M. N.; Dietrich, S.; Tasinkevych, M. Self-Propulsion of a Catalytically Active Particle near a Planar Wall: From Reflection to Sliding and Hovering. *Soft Matter* **2015**, *11*, 434−438.

(50) Das, S.; Garg, A.; Campbell, A. I.; Howse, J.; Sen, A.; Velegol, D.; Golestanian, R.; Ebbens, S. J. Boundaries Can Steer Active Janus Spheres. *Nat. Commun.* **2015**, *6*, 8999.

(51) Ma, X.; Hahn, K.; Sanchez, S. Catalytic Mesoporous Janus Nanomotors for Active Cargo Delivery. *J. Am. Chem. Soc.* **2015**, *137*, 4976−4979.

(52) Lee, T.-C.; Alarcón-Correa, M.; Miksch, C.; Hahn, K.; Gibbs, J. G.; Fischer, P. Self-Propelling Nanomotors in the Presence of Strong Brownian Forces. *Nano Lett.* **2014**, *14*, 2407−2412.

(53) Wilson, D. A.; Nolte, R. J. M.; van Hest, J. C. M. Autonomous Movement of Platinum-Loaded Stomatocytes. *Nat. Chem.* **2012**, *4*, 268−274.

(54) Dunderdale, G.; Ebbens, S.; Fairclough, P.; Howse, J. Importance of Particle Tracking and Calculating the Mean-Squared Displacement in Distinguishing Nanopropulsion from Other Processes. *Langmuir* **2012**, *28*, 10997−11006.

(55) Ma, X.; Hortelão, A.; Patiño, T.; Sánchez, S. Enzyme Catalysis To Power Micro/Nanomachines. *ACS Nano* **2016**, *10*, 9111−9122.

(56) Ma, X.; Sanchez, S. A Bio-Catalytically Driven Janus Mesoporous Silica Cluster Motor with Magnetic Guidance. *Chem. Commun.* **2015**, *51*, 5467−5470.

(57) Ma, X.; Jannasch, A.; Albrecht, U.-R.; Hahn, K.; Miguel-López, A.; Schäffer, E.; Sánchez, S. Enzyme-Powered Hollow Mesoporous Janus Nanomotors. *Nano Lett.* **2015**, *15*, 7043−7050.

(58) Ma, X.; Wang, X.; Hahn, K.; Sánchez, S. Motion Control of Urea-Powered Biocompatible Hollow Microcapsules. *ACS Nano* **2016**, *10*, 3597−3605.

(59) Orozco, J.; García-Gradilla, V.; D'Agostino, M.; Gao, W.; Cortés, A.; Wang, J. Artificial Enzyme-Powered Microfish for Water-Quality Testing. *ACS Nano* **2013**, *7*, 818−824.

(60) Wu, Z.; Lin, X.; Zou, X.; Sun, J.; He, Q. Biodegradable Protein-Based Rockets for Drug Transportation and Light-Triggered Release. *ACS Appl. Mater. Interfaces* **2015**, *7*, 250−255.

(61) Dey, K. K.; Zhao, X.; Tansi, B. M.; Méndez-Ortiz, W. J.; Córdova-Figueroa, U. M.; Golestanian, R.; Sen, A. Micromotors Powered by Enzyme Catalysis. *Nano Lett.* **2015**, *15*, 8311−8315.

(62) Abdelmohsen, L. K. E. A.; Nijemeisland, M.; Pawar, G. M.; Janssen, G.-J. A.; Nolte, R. J. M.; van Hest, J. C. M.; Wilson, D. A. Dynamic Loading and Unloading of Proteins in Polymeric Stomatocytes: Formation of an Enzyme-Loaded Supramolecular Nanomotor. *ACS Nano* **2016**, *10*, 2652−2660.

(63) Bunea, A.-I.; Pavel, I.-A.; David, S.; Gáspár, S. Sensing Based on the Motion of Enzyme-Modified Nanorods. *Biosens. Bioelectron.* **2015**, *67*, 42−48.

(64) Ma, X.; Hortelão, A.; Miguel-López, A.; Sánchez, S. Bubble-Free Propulsion of Ultrasmall Tubular Nanojets Powered by Biocatalytic Reactions. *J. Am. Chem. Soc.* **2016**, *138*, 13782−13785.

(65) Schattling, P.; Thingholm, B.; Städler, B. Enhanced Diffusion of Glucose-Fueled Janus Particles. *Chem. Mater.* **2015**, *27*, 7412−7418.

(66) Khalil, I. S. M.; Magdanz, V.; Sanchez, S.; Schmidt, O. G.; Misra, S. Biocompatible, Accurate, and Fully Autonomous: A Sperm-Driven Micro-Bio-Robot. *J. Micro-Bio Robot.* **2014**, *9*, 79−86.

(67) Magdanz, V.; Medina-Sanchez, M.; Chen, Y.; Guix, M.; Schmidt, O. G. How to Improve Spermbot Performance. *Adv. Funct. Mater.* **2015**, *25*, 2763−2770.

(68) Magdanz, V.; Guix, M.; Hebenstreit, F.; Schmidt, O. G. Dynamic Polymeric Microtubes for the Remote-Controlled Capture, Guidance, and Release of Sperm Cells. *Adv. Mater.* **2016**, *28*, 4084−4089.

(69) Medina-Sánchez, M.; Schwarz, L.; Meyer, A. K.; Hebenstreit, F.; Schmidt, O. G. Cellular Cargo Delivery: Toward Assisted Fertilization by Sperm-Carrying Micromotors. *Nano Lett.* **2016**, *16*, 555−561.

(70) Tottori, S.; Zhang, L.; Qiu, F.; Krawczyk, K. K.; Franco-Obregón, A.; Nelson, B. J. Magnetic Helical Micromachines: Fabrication, Controlled Swimming, and Cargo Transport. *Adv. Mater.* **2012**, *24*, 811−816.

(71) The Human Microbiome Consortium. Structure, Function and Diversity of the Healthy Human Microbiome. *Nature* **2012**, *486*, 207−214.

(72) Taherkhani, S.; Mohammadi, M.; Daoud, J.; Martel, S.; Tabrizian, M. Covalent Binding of Nanoliposomes to the Surface of Magnetotactic Bacteria for the Synthesis of Self-Propelled Therapeutic Agents. *ACS Nano* **2014**, *8*, 5049−5060.

(73) Behkam, B.; Sitti, M. Bacterial Flagella-Based Propulsion and On/off Motion Control of Microscale Objects. *Appl. Phys. Lett.* **2007**, *90*, 023902.

(74) Sahari, A.; Traore, M. A.; Scharf, B. E.; Behkam, B. Directed Transport of Bacteria-Based Drug Delivery Vehicles: Bacterial Chemotaxis Dominates Particle Shape. *Biomed. Microdevices* **2014**, *16*, 717−725.

(75) Kim, D.; Liu, A.; Diller, E.; Sitti, M. Chemotactic Steering of Bacteria Propelled Microbeads. *Biomed. Microdevices* **2012**, *14*, 1009−1017.

(76) Zhuang, J.; Wright Carlsen, R.; Sitti, M. pH-Taxis of Biohybrid Microsystems. *Sci. Rep.* **2015**, *5*, 11403.

(77) Park, S. J.; Bae, H.; Kim, J.; Lim, B.; Park, J.; Park, S. Motility Enhancement of Bacteria Actuated Microstructures Using Selective Bacteria Adhesion. *Lab Chip* **2010**, *10*, 1706−1711.

(78) Stanton, M. M.; Simmchen, J.; Ma, X.; Miguel-López, A.; Sánchez, S. Biohybrid Janus Motors Driven by Escherichia Coli. *Adv. Mater. Interfaces* **2016**, *3*, 1500505.

(79) Park, S. J.; Park, S.-H.; Cho, S.; Kim, D.-M.; Lee, Y.; Ko, S. Y.; Hong, Y.; Choy, H. E.; Min, J.-J.; Park, J.-O.; Park, S. New Paradigm for Tumor Theranostic Methodology Using Bacteria-Based Micro-robot. *Sci. Rep.* **2013**, *3*, 3394.

(80) Fernandes, R.; Zuniga, M.; Sassine, F. R.; Karakoy, M.; Gracias, D. H. Enabling Cargo-Carrying Bacteria via Surface Attachment and Triggered Release. *Small* **2011**, *7*, 588−592.

(81) Parmar, J.; Ma, X.; Katuri, J.; Simmchen, J.; Stanton, M. M.; Trichet-Paredes, C.; Soler, L.; Sanchez, S. Nano and Micro Architectures for Self-Propelled Motors. *Sci. Technol. Adv. Mater.* **2015**, *16*, 014802.